An MRI Investigation of the Effect of Active Site Mutant DDAH1 in C6 Glioma Xenografts In Vivo

J. K. Boult[1], S. Walker-Samuel[1], Y. Jamin[1], J. M. Leiper[2], G. S. Whitley[3], and S. P. Robinson[1]

[1]CRUK and EPSRC Cancer Imaging Centre, The Institute of Cancer Research and Royal Marsden NHS Trust, Sutton, Surrey, United Kingdom, [2]MRC Clinical Sciences Centre, Faculty of Medicine, Imperial College London, London, United Kingdom, [3]Department of Basic Medical Sciences, St. Georges, University of London, London, United Kingdom

Introduction

Dimethylarginine dimethylaminohydrolase (DDAH) metabolizes the endogenous inhibitor of nitric oxide synthesis, asymmetric dimethylarginine (ADMA), indirectly leading to an increase in nitric oxide [1]. Evidence suggests that nitric oxide (NO) is a crucial signalling molecule and regulator of angiogenesis, and stimulates the expression of VEGF [2]. It has previously been shown that constitutive overexpression of DDAH1 in C6 glioma xenografts results in increased tumour growth, angiogenesis and elevated VEGF secretion [3]. To address whether this DDAH1-mediated tumour growth is reliant upon its enzymatic activity, stable cell lines that express an active site mutant of DDAH1 incapable of metabolizing ADMA were created. We hypothesized that, in the absence of enzymatic activity, the DDAH1 mutant would elicit similar growth and vascular properties to control C6 tumours. The vascular phenotype was interrogated *in vivo* using diffusion weighted and dynamic contrast enhanced (DCE) MRI.

Methods

Tumour model: C6 rat glioma cell lines were genetically modified to stably overexpress wild-type rat DDAH1 (D27), active site mutant rat DDAH1 (DM1, DM2, DM3) or vector only (M8, control). $2x10^6$ C6 cells were inoculated subcutaneously on the flank of female NCr nude mice.

MRI measurements: A diffusion-weighed spin-echo sequence (T_R=1500ms, 5 b-values from 6 to 1000s/mm^2, 1 average) was used to determine the apparent diffusion coefficient (ADC) of D27, DM1 and M8 tumours, providing a measure of the rate of extracellular water diffusion, and which relates to tissue cellularity. DCE-MRI data were then acquired using an inversion recovery (IR) true-FISP sequence with one baseline scan (T_I=130-2592ms, 20 inversion times, T_R=4ms, T_E=2ms, 12 averages) and 75 dynamic scans (T_I=130-1037ms, 8 inversion times, T_R=4ms, T_E=2ms, temporal resolution=9s, 2 averages) prior to and following administration of 0.1mmol/kg Gd-DTPA (Magnevist, Schering) i.v.. This provided estimates of K^{trans} (dependent on permeability, blood flow and blood volume) and v_e (fraction of extra-vascular, extracellular volume).

Data analysis: Diffusion data were fitted using a Bayesian maximum *a posteriori* approach that took into account the Rician distribution of noise in magnitude MR data and provided estimates of the native ADC [4]. IR-trueFISP data were fitted using a similar approach, which also utilised the dual relaxation rate sensitivity (T_1 and T_2) of the IR-trueFISP sequence and incorporated the Tofts and Kermode pharmacokinetic model [5]. This provided estimates of K^{trans}, v_e and native T_1 and T_2. All data were fitted on a pixel-by-pixel basis using in-house software (ImageView). The median value of each parameter in each tumour was measured.

Histology, VEGF Expression and DDAH Activity: Mice were administered with 60mg/kg pimonidazole (a hypoxia marker) i.p., followed by the perfusion marker Hoechst 33342 (15mg/kg) i.v.. The percentage pimonidazole adduct formation and Hoechst 33342 uptake were determined and quantified by fluorescence microscopy. Haematoxylin and eosin staining was also performed to quantify necrosis. Tumour homogenates were assayed for VEGF expression by ELISA, and for DDAH activity by quantitation of conversion of ^{14}C-L-NMMA to ^{14}C-citrulline.

Results & Conclusions

The growth rates of tumours derived from three separate C6 cell lines overexpressing active site mutant DDAH1 (DM, mean doubling time 2.9 days) were significantly faster than tumours derived from mock-transfected C6 cells (M8, 4.5 days, $p<0.01$), but not as fast as tumours overexpressing wild-type DDAH1 (D27, 2.5 days, NS). A significantly higher ADC was determined in the M8 tumours compared to D27 tumours, and higher native T_1 and T_2 times in the M8 tumours than both D27 and DM1 tumours. Together these data are consistent with a reduced fraction of bound water in the M8 tumours and increased necrosis, which was confirmed histologically from H&E stained sections (Figure 1 and Table 1).

VEGF expression in the DM tumours (mean 793pg/mg) was significantly lower than that of D27 tumours (2502pg/mg, $p<0.05$), but not significantly different to M8 tumours (709pg/mg). Despite these differences in VEGF expression, no significant differences in K^{trans} or v_e were observed between the 3 tumour groups. This highlights the challenges of interpreting the compound imaging biomarker K^{trans} in tumours. Hoechst 33342 uptake in D27 tumours was significantly greater than in M8 tumours (D27 5.9%, M8 4.0%, $p<0.05$), as previously reported [3], but no significant difference was observed between DM1 and either M8 or D27 tumours. DM1 tumours were significantly less hypoxic than D27 gliomas, as were M8 tumours (Table 1). DDAH activity was significantly higher in both D27 and DM1 tumours than control M8 tumours (315% and 196% of M8 ^{14}C-citrulline production, respectively, $p<0.001$) and higher in D27 than DM1 tumours ($p<0.0001$).

Tumours expressing mutant DDAH1 exhibited an intermediate proliferative phenotype between control and wildtype DDAH1 expressing tumours *in vivo*. This is consistent with ADMA being able to associate with its active site but not be metabolized, yet still removing free ADMA from inhibiting nitric oxide synthesis, or an ADMA-independent function of mutant DDAH1 [6]. *In vivo* the increased DDAH activity in DM1 tumours relative to control M8 tumours, which was not seen *in vitro*, may be as a result of DDAH expression in non-tumour cells, for example infiltrating macrophages and vascular endothelial cells, within the tumour [7, 8].

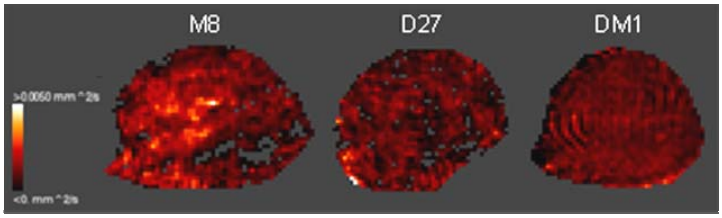

Figure 1. Representative ADC maps from control (M8), wild type DDAH1 expressing (D27) and mutant DDAH1 expressing (DM1) C6 xenografts.

Imaging Biomarker	M8	D27	DM1
ADC (x10^{-6} mm^2/s)	977 ± 82	741 ± 50 $^{\#}$	898 ± 97
Native T_1 (ms)	2313 ± 19	2171 ± 36 $^{\#}$	2142 ± 60 $^{\#}$
Native T_2 (ms)	102 ± 2.7	71 ± 3.0 $^{\#\#\#}$	82 ± 2.5 $^{\#\#}$ *
K^{trans} (min^{-1})	0.045 ± 0.009	0.037 ± 0.01	0.034 ± 0.005
v_e	0.266 ± 0.09	0.487 ± 0.14	0.388 ± 0.14
Necrosis (%)	66 ± 5.1	22 ± 8.8 $^{\#}$	59 ± 3.5 *
Pimonidazole (%)	19 ± 1.4	27 ± 1.8 $^{\#}$	16 ± 2.6 *

Table 1. Summary of the quantitative MRI and histological biomarkers. Mean ± 1sem. n>4, $^{\#}p<0.05$, $^{\#\#}p<0.01$, $^{\#\#\#}p<0.001$ relative to M8. *$p<0.05$ relative to D27.

References.

[1] Ogawa T. *et al*. (1989*) J Biol Chem* 264:10205-9. [2] Papapetropoulos A. *et al*. (1997) *J Clin Invest* 100:3131-9. [3] Kostourou V. *et al.* (2002) *Br J Cancer* 87:673-80. [4] Walker-Samuel S. *et al.* (2009) *Magn Reson Med* 62:420-9. [5] Walker-Samuel S. *et al*., (2009) *Proc Intl Soc Mag Reson Med* 17:abstract 5595. [6] Hasegawa K. *et al*. (2006) *Arterioscler Thromb Vasc Biol* 26:1488-94. [7] Kimoto M. *et al*. (1993) *Arch Biochem Biophys* 300:657-62. [8] Hecker M. *et al*. (1990) *Biochem Biophys Res Commun* 167:1037-43.

Acknowledgments

We acknowledge the support received for the CRUK and EPSRC Cancer Imaging Centre in association with the MRC and Department of Health (England) (grants C1060/A10334 and C16412/A6269), the Biotechnology and Biological Sciences Research Council (grant S20430), NHS funding to the NIHR Biomedical Research Centre and The Royal Society.